Localization of ultrasound in 2D phononic crystal with randomly oriented asymmetric scatterers ⊘ F FREE

Jyotsna Dhillon ; Andrey Bozhko; Ezekiel Walker ; Arup Neogi ; Arkadii Krokhin ✉

Check for updates
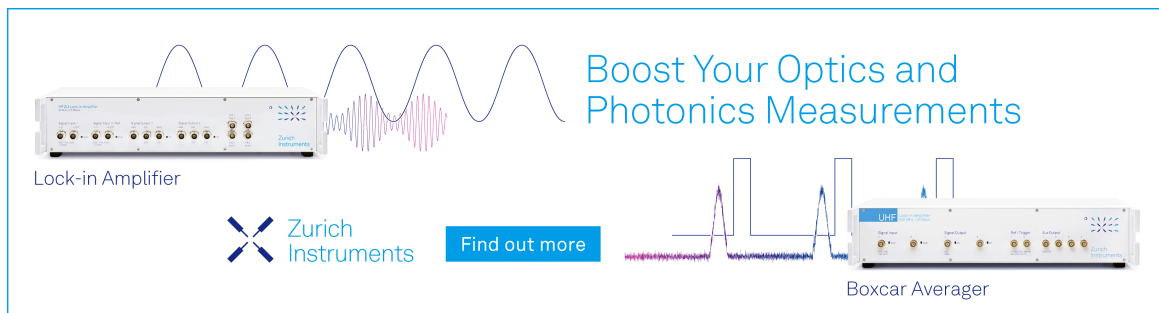
CHORUS

View Online

Export Citation

Localization of ultrasound in 2D phononic crystal with randomly oriented asymmetric scatterers SCI F

Jyotsna Dhillon,[1] ID Andrey Bozhko,[1] Ezekiel Walker,[2] ID Arup Neogi,[1] ID and Arkadii Krokhin[1,a] ID

AFFILIATIONS

[1]Department of Physics, University of North Texas, 1155 Union Circle #311277, Denton, Texas 76203, USA
[2]Echonovus Inc., 1800 S Loop 288, Denton, Texas 76205, USA

Note: This paper is part of the Special Topic on Acoustic Metamaterials 2021.
[a]**Author to whom correspondence should be addressed:** arkady@unt.edu

ABSTRACT

A phononic crystal of aluminum rods with an asymmetric cross section in water is used for the study of Anderson localization of sound. Due to asymmetry, these scatterers may be arranged in three different configurations: a periodic 2D structure, a random structure with 2D disorder, and a random structure with 1D disorder. The last configuration where the rods are equally oriented within the columns and disoriented along the rows is fabricated for the experimental study of 1D Anderson localization in the 2D random system. An exponentially weakening transmission of the ultrasound is demonstrated for the waves propagating along the direction of disorder. In the perpendicular direction where the scatterers are ordered, sound propagates as an extended (delocalized) wave. The localization length is controlled by the degree of disorder. For weak disorder, when orientations of the rods weakly fluctuate around a given direction, Thouless's theoretical prediction for the scaling of the Lyapunov exponent with disorder is experimentally observed for a mode within the transmission band. For the sound mode close to the band edge, anomalous scaling is confirmed.

I. INTRODUCTION

A set of disordered scatterers, depending on its strength and dimensionality, may lead to Anderson localization of waves. Anderson localization,[1] or strong localization, is a regime when the diffusive propagation of a quantum particle or a wave is not possible due to the destructive interference of backscattered and incoming waves. This results in the localization of an incoming signal within a finite region, termed the *localization length l*, and in the exponential decay of the signal outside of this region. If at a given frequency ω, the length of the sample L adequately exceeds the localization length $l(\omega)$, the amplitude of the transmitted signal $\sim \exp(-L/l)$ becomes so weak that the disordered medium can be considered nontransparent (insulator). It is well known that for one-dimensional (1D) and two-dimensional (2D) systems, any weak disorder localizes the incoming wave.[2] For 2D weakly disordered systems, the localization length grows exponentially with the mean free path, making it challenging to experimentally observe localized states since it requires an enormously large, weakly disordered system. Localization in 3D systems requires the strength of disorder to exceed some critical value, at which point a

metal–insulator transition becomes possible. For light, the effect of Anderson localization was observed for different types of disorders in 1D (and quasi-1D),[3–5] 2D,[6,7] and 3D systems.[8] Modern reviews on the current state of the problem of localization of light can be found in Refs. 9 and 10.

There are relatively fewer reports on the localization of sound. Some signatures of localization of ultrasound in a polymer elastic disk subjected to liquid–solid temperature transition were reported in Ref. 11. The authors measured signal attenuation and change of the sound phase velocity in a sample where random scatterers were the nucleation centers formed in the process of solidification. Approximately at the same time, the localization of elastic vibrations of an aluminum plate with randomly distributed slits was observed.[12] One-dimensional localization of torsion and flexural elastic waves in solid rods with randomly distributed masses was reported in Refs. 13 and 14. An extended study of the localization of sound waves in a network of elastic spheres was done in Ref. 15. Several signatures of localization have been reported, including the comparison of the microstructure of the localized and delocalized (extended) states and some results of the observation of transverse Anderson localization

in three dimensions. Later on, an additional experiment on transverse localization was performed using a multichannel waveguide with random coupling between discrete acoustic channels.[16]

Here, we propose the use of a phononic crystal with randomly oriented asymmetric aluminum rods embedded in viscous liquid (water) to observe the localization of ultrasound. While this arrangement of scatterers is two-dimensional, it is easy to obtain a one-dimensional disorder if all the rods are equally oriented within the columns but randomized along the rows (see Fig. 1). Due to the difference in symmetry, this arrangement of scatterers behaves like an ordered system if sound propagates along the columns and as a 1D disordered structure if sound propagates along the rows. The level of disorder is controlled by the angle of orientation of the rods in each column. Since all the rods are equal, they can be arranged in a periodic phononic crystal if all the rods are equally oriented. Such a configuration was used in Refs. 17 and 18 for the demonstration of acoustic nonreciprocity in a system of anisotropic scatterers in a viscous environment. The rods behave like a 2D disordered structure if the order along the columns is broken and all the scatterers are randomly oriented. This last configuration is suitable for the study of 2D Anderson localization. However, such study requires much longer samples. We consider structures with a strong and weak 1D disorder. For the latter case, which was analyzed by Thouless,[19] it is confirmed experimentally and numerically that the inverse localization length l^{-1} scales as the variance of the fluctuating angle of the orientation if the frequency fits a transmission band. However, if the frequency approaches a bandgap, we, for the first time, experimentally observe anomalous scaling.

Transmission through a two-dimensional elastic phononic crystal with isotropic scatterers with one-dimensional disorder was numerically analyzed in Refs. 20 and 21. Random fluctuations were introduced through random perturbation in the filling fraction along the direction of disorder. The shape and the orientation of the square scatterers were not perturbed. The localization of elastic waves was reported. Also, the fragmentation of the band structure for the quasi-periodic sequence of columns was numerically confirmed.

II. ANALYSIS OF TRANSMISSION SPECTRA

The experiments on sound transmission were performed using the sample shown in Fig. 1. It contains 9×9 aluminum rods arranged in a square lattice with period $a = 5.5$ mm. Each rod has the same cross section in a form of a circular sector of a radius of 2.2 mm with an angle of 120°. The rods are equally oriented within the columns and randomly oriented along the rows. Either the number of columns or the number of rows was gradually reduced from 9 to 1 in the experiments where transmission was measured as a function of the sample length.

Transmission spectra were recorded along the x-(disordered) and y-(ordered) directions using two identical Olympus V301 0.5 MHz 1 in. unfocused immersion transducers in a bi-static, thru-transmission setup. The measurement was performed by centering the sample between the two transducers, with one transducer
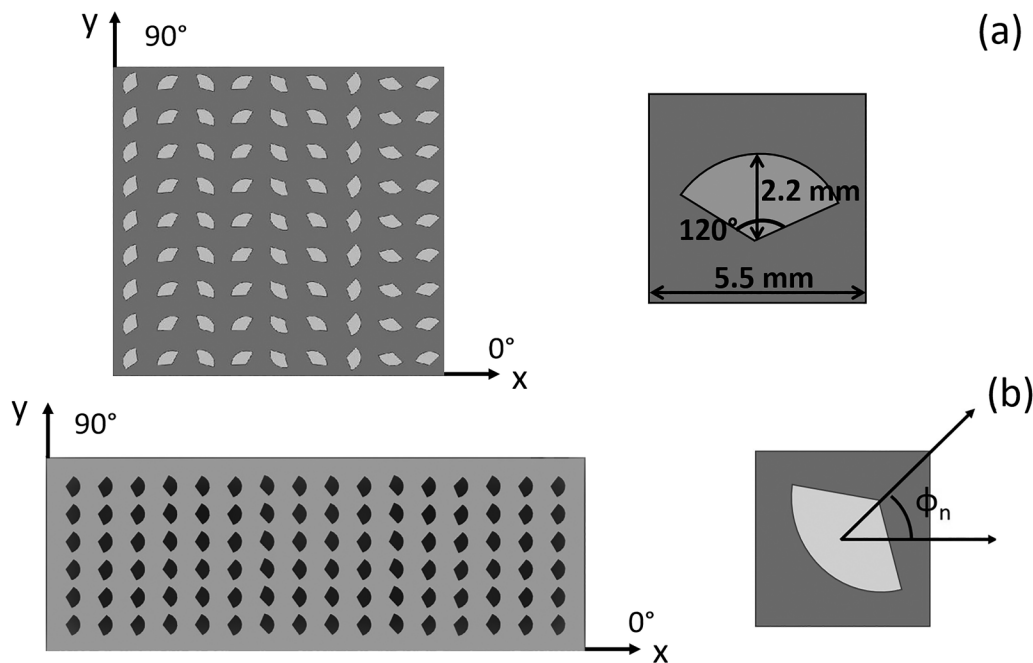
FIG. 1. (a) Disordered phononic crystal of 9×9 aluminum rods used in the experiments on sound transmission. Along the x axis, the rods are completely disoriented producing strong disorder. The right panel shows the parameters of the unit cell. The direction along the positive x (y) axis corresponds to 0° (90°). (b) Weakly disordered phononic crystal of 16×6 aluminum rods with $\sigma = 6°$. The right panel shows the orientation of a rod in a disordered structure.

19 April 2024 13:47:36

connected to a signal generator and the other connected to a Tektronix MDO 3024b Spectrum Analyzer. The transducers are placed in a manner that they were within 1.5 mm of both the incident and transmission sides of the crystal, respectively. Spectra were obtained by sweeping the function generator in a continuous wave mode over the full bandwidth of the transducers at a constant input voltage of 20Vpp.

To obtain the transmission spectral behavior as dependent on distance, spectra were recorded for 9-1 layers (e.g., 9×9, $9 \times 8, \ldots, 9 \times 1$) along the direction of propagation in both the x and y directions. For each representation of the sample, the transmission was recorded with both the sample present and the sample removed for a baseline. The difference between the signals received for the sample and the baseline measured in dB was used for analysis. All measurements were performed at the same room temperature in a tank filled with de-ionized water as the ambient medium for the sample. The design of the metamaterial was based on the frequency range of the transducers, available hardware to construct the metamaterials, and modeled results. Though the application of traditional Bloch wave dynamics is not ideal due to the asymmetry of the scatterers and the layout of the periodicity, the design of the structure was such that the lower end of the frequency range fits the first frequency gap.

The propagation of sound through the crystal was also simulated numerically. Throughout all the numerical simulations performed, the aluminum rods were treated as elastic objects with the appropriate elastic moduli. The frequency-domain simulations were performed using COMSOL Multiphysics software. The behavior of the water environment was governed by the Linearized Navier–Stokes module from the Linearized Navier–Stokes (frequency domain) physics, and that of the aluminum scatterers—by the Linear Elastic Material model from the Solid Mechanics physics. The density, Young's modulus, and Poisson's ratio for aluminum used in the model were $2700 \, \text{kg/m}^3$, $70 \times 10^9 \, \text{Pa}$, and 0.33, respectively. The parameters used for water are an elastic bulk modulus of $2.15 \times 10^9 \, \text{Pa}$, a density of $10^3 \, \text{kg/m}^3$, a shear viscosity of $0.001 \, \text{Pa s}$, and a bulk viscosity of $0.003 \, \text{Pa s}$. The no-slip boundary condition was applied at the surfaces of the rods. The accuracy of numerical calculations was selected sufficiently high in order to resolve the viscous layer formed around each solid scatterer. The thickness of the layer $\delta = \sqrt{2\eta/\rho\omega}$ at the highest frequency used in the experiment ($\omega/2\pi = 600 \, \text{kHz}$) is about $1 \, \mu\text{m}$ that is much less than the wavelength $\lambda \approx 2.5 \, \text{mm}$. The mesh used in numerical calculations of the transmission spectra was $\delta/6$ within the boundary layers and it gradually increases away from the boundary. Decreasing the mesh size practically does not change the transmission spectra, indicating sufficient accuracy of our numerical results.

A. Spectra for sound propagating along the direction of periodicity

The structure in Fig. 1 possesses translational symmetry in the vertical direction (along the y axis). This symmetry, however, is not the same as the symmetry of a crystal periodic in both directions. The Bloch theorem for translation by period a along y states that pressure $p(x, y + a) = e^{ik(x)a}p(x, y)$. Here, the Bloch vector $k(x)$ is not the same for all the columns but it changes with x-coordinate.
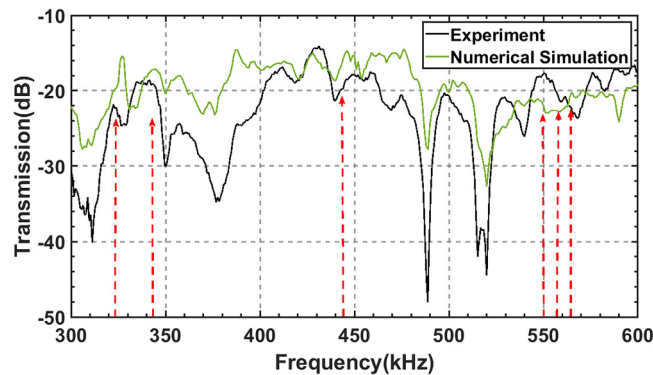

FIG. 2. The transmission spectra, experimental and numerical, of the 6×9 phononic crystal for sound waves propagating along the y axis (along the ordered structure of six rows). Red vertical arrows show the resonant frequencies of a single aluminum rod in the water.

Therefore, the propagating monochromatic wave, $p \sim e^{-i\omega t}$, cannot be characterized by the dispersion relation of a standard type, $\omega = \omega(k)$. Due to disorientation of the rods, diffraction at a set of scatterers does not lead to a regular pattern typical for a crystal, resulting in the transmission spectra in Fig. 2 exhibiting the irregular sequence of passing bands and gaps.

Each rod is a resonator with a set of frequencies marked by vertical red arrows in Fig. 2. Due to coupling to water, the resonances are of finite width and the broadening quickly increases with frequency. The lowest three resonances are well-resolved. There are pronounced minima near these resonances due to enhanced scattering and absorption of sound. At higher frequencies, the widths of the resonances become comparable to the spacing between the resonances; therefore, the corresponding minima in transmission disappear. Numerically calculated positions of resonances are slightly shifted with respect to experimentally observed minima because of finite interactions between the rods. The frequencies near these resonances should be avoided when considering Anderson localization for the reason that it would not be possible to rule out the additional exponential decay due to the resonant excitation of the rods leading to anisotropic resonant scattering. This resonant scattering is irrelevant to the backscattering, which is a source of Anderson localization. Similar features in the transmission spectrum were reported in Ref. 15.

Other minima and maxima in the transmission spectrum originate from multiple scattering and their positions are irregular. The experimental graph reproduces most of the main features predicted numerically, although experimental transmission is lower than numerically calculated. This difference is due to the presence of the surface roughness of the rods. The size of the surface roughness is comparable with the thickness of the viscous boundary layer δ. Viscous dissipation is proportional to the real area of the scatterers. Since the rough surface has a larger area than the corresponding flat surface, the experimental transmission turns out to be less than numerically calculated. It is worthwhile to estimate dissipative losses due to the viscosity of water. In pure water, the decay length

$l_0(\omega) = \frac{2\rho c^3}{\omega^2} \left[\frac{4}{3}\eta + \xi \right]^{-1}$ of a plane sound wave of frequency $\omega/2\pi = 500$ kHz ($c \approx 1.5 \times 10^3$ m/s) is about 200 m. It means that the dissipative losses in pure water at the distances compared to the sizes of our samples, which do not exceed 10 cm, are negligible. However, the sound wave propagates not in pure water but through a dense set of solid rods. A viscous boundary layer of thickness δ is formed near each rod. Dissipation of acoustic energy occurs within these boundary layers where the gradients of velocity are much greater than in pure water. Due to strongly enhanced dissipation in sound wave reflection from a solid boundary (so-called Konstantivov's effect[22]), the propagation length of sound in a phononic crystal is strongly reduced.

The dissipative decay length of sound in the 2D phononic crystal was calculated in Ref. 23. While it was shown that the exact value of the viscous decay coefficient $\gamma(\omega)$ depends essentially on the shape of the rods, a rough estimate can be obtained as follows. Reflecting from a solid plane, a sound wave with energy density E losses part Q/E of its acoustic energy, where Q is the viscous losses per unit volume. The dissipative losses can be estimated as $Q/E \sim c^{-1}\sqrt{\omega\eta/\rho}$, where η and ρ are, respectively, the shear viscosity and the mass density of the fluid (see, e.g., Ref. 22). This result applied to a 2D unit cell of typical size a containing cylindrical rod of circumference L gives an extra factor L/a. The latter factor is estimated as $L/a \sim \sqrt{f}$, where f is the filling fraction of the unit cell. Thus, for the part of energy lost due to viscosity, we get $Q/E \sim c^{-1}\sqrt{f\omega\eta/\rho}$. The decay coefficient of a plane wave $\gamma(\omega)$ is given by the part of energy lost per unit length, which leads to the following result for the decay coefficient:

$$\gamma(\omega) = \frac{Q}{aE} \sim \frac{1}{ca}\sqrt{\frac{f\eta\omega}{\rho}}. \tag{1}$$

The enhancement of dissipation in phononic crystal as compared to pure water is

$$\gamma(\omega)l_0(\omega) \sim \frac{c^2}{a}\sqrt{\frac{f\rho}{\eta\omega^3}}. \tag{2}$$

Substituting the parameters of the phononic crystal shown in Fig. 1, we obtain that the propagation length is reduced by ~30 times as compared to that in pure water at a frequency of 500 kHz. There is a numerical factor missing in Eq. (2), which is defined by the exact geometry of the unit cell. Using the method proposed in Ref. 23, we obtained that the missing numerical factor is close to 10. As a result, we conclude that the decay length of sound due to viscosity, $1/\gamma(\omega)$, does not exceed 1 m. While the decay length is still greater than the length of the sample, $L = 88$ mm, the dissipative attenuation of sound amplitude is about 10%.

We attribute additional dissipation of sound to the presence of microscopic roughnesses at the cylindrical surfaces of the rods. The typical size of roughnesses at the surface of the aluminum sample is about a few micrometers. The thickness of the viscous layer δ is about 1 μm or greater. This means that dissipation occurs not at a flat solid-fluid boundary but at a statistically rough surface. The area of a rough surface significantly exceeds the area of the

corresponding flat area giving rise to much stronger dissipation. Similar enhancement of dissipation was reported also for the periodic phononic crystal.[17] The microscopic roughnesses cannot be resolved by the sound wave with the wavelength of a few milliliters, and they have very little effect on diffusive scattering of sound. Note that dissipative losses strongly depend on the distribution of the local velocities of fluid, which changes essentially with frequency. Therefore, the difference between experimental and simulated transmission does not remain the same but changes with frequency.

B. Spectra for sound propagating along the direction of disorder

A sound wave propagating along the x axis suffers from strong random scattering and the transmission spectra in Fig. 3 do not show any regular structure. It is clear that the positions of the transmission bands and gaps in the lower panel do not correspond to the positions of those in the upper panel. The reason is the disordered orientation of the scatterers, which leads to a very different diffraction pattern than the one obtained from an ordered crystal. The band structure shown in the lower panel of Fig. 3 is for the sound wave propagating along the axis of symmetry of the scatterers (see the insert). This wave excites only symmetric (even) modes. The dispersion curves of these modes are shown by black lines.
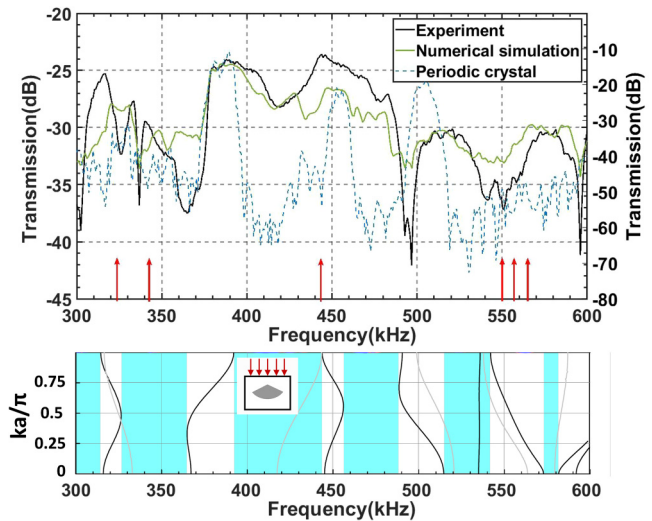

FIG. 3. Upper panel: the transmission spectra (with left vertical axis) of 9×6 phononic crystal for the sound wave propagating along the x axis (along disordered structure of six columns). The experimentally measured transmission through a long (16×6) periodic phononic crystal is shown by the dashed line with the right vertical axis. Red vertical arrows show the resonant frequencies of a single aluminum rod in the water. Lower panel: the band structure of the phononic crystal with inviscid water background for the sound wave propagating along the direction of broken P-symmetry.[17] Passing bands corresponding to even (odd) eigenmodes are shown by black (grey) lines. Regions of gaps between the even zones are shaded. The direction of propagation of sound wave is shown in the inset.
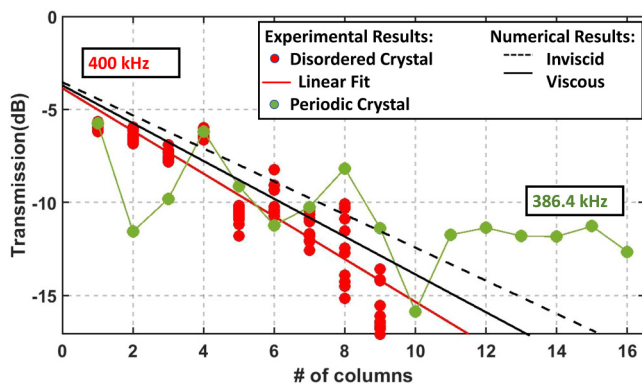
The antisymmetric (odd) modes (shown by gray lines) cannot be excited. It is a deaf mode for this direction of propagation. However, in a disordered crystal, the antisymmetric vibrations are equally excited. This also affects the transmission spectrum. The transmission spectra measured for the corresponding *periodic* phononic crystal are shown by the dashed line. The positions of the transmission bands and gaps coincide well with those calculated for the infinite crystal, while the band edges are broadened due to radiative and dissipative losses. While the periodic structure is longer, it contains 16 periods against 6, it transmits sound better than the disordered one. The same is true for the insulation of sound within the bandgaps.

III. LOCALIZATION LENGTH

Anderson localization of sound propagating along the direction of disorder was observed in the experiment with samples of different lengths L. The localization length is a self-averaged parameter of a disordered system calculated as

$$l^{-1}(\omega) = \frac{2}{L}\left\langle \ln\frac{I_0}{I(L,\omega)}\right\rangle, \tag{3}$$

where $I(L,\omega)$ is the intensity of transmitted sound and averaging is taken over a statistical ensemble of disordered samples. In the experiment and numerical simulations, the latter averaging is replaced by averaging over 11 frequencies lying within a symmetric narrow window of 8 kHz centered at frequency $\omega/2\pi$. The linear fit of the average logarithm of the transmission coefficient vs sample length is plotted in Fig. 4 for frequency $\omega/2\pi = 400$ kHz. This frequency is away from the resonances of individual rods and the transmission coefficient near 400 kHz does not exhibit any
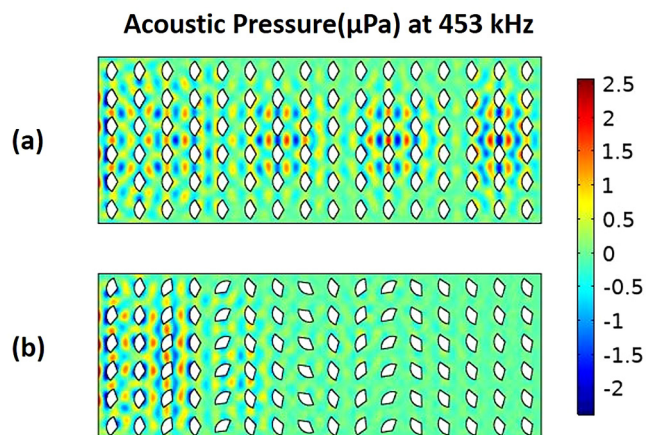
anomaly. It is important that in the vicinity of this frequency, the transmission coefficient is a relatively flat function. The latter can be considered as "ergodic property" that allows one to replace averaging over statistical ensemble by averaging over a narrow interval of frequencies. Note that for the periodic crystal, this frequency fits the bandgap (see Fig. 3). Linear decay of the average transmission (in dB) with sample length is a signature of Anderson localization. The slope of the lines in Fig. 4 gives the following values for the localization length measured in lattice period ($a = 5.5$ mm): $l_{exp} = 7.64$ and $l_{num} = 8.36$ for experimental and numerical results, respectively. Experimental results give stronger localization since there are some factors such as surface roughness of the rods and radiation losses that lead to faster decay of the signal experimentally but are ignored in the theory.

Green dots in Fig. 4 show the results obtained for a periodic 16×6 sample at a frequency of 386.4 kHz. This frequency is in the middle of a transmission band if sound propagates along the direction of broken P-symmetry (see the lower panel in Fig. 3). Transmission through the periodic crystal oscillates with the sample length. These oscillations are of the same nature as oscillations of transmission through a finite-thickness homogeneous slab. They originate from interference between the direct wave and the wave reflected from the back interface. In an ideal case of the absence of scattering and viscous losses, the transmission oscillates without decay. In the experiment, we observe decaying oscillations but the decay is much slower than the linear decay observed for the disordered sample. This is a signature of the extended nature of the eigenstates of the periodic crystal.

If sound propagates along the direction of disorder, these oscillations are much less manifested. They are seen also in the plot of transmission along the direction of order (see Fig. 6). The amplitude of these oscillations decreases after averaging over a narrow frequency interval. Oscillations vanish after averaging over the statistical ensemble, resulting in a linear decay of sound intensity with the sample length as it is shown by two black lines in Fig. 4.

FIG. 4. Transmission coefficient (in dB) along the direction of disorder (x axis) as a function of the sample length. The slope of the linear fit obtain from experimental and numerical results is proportional to the inverse localization length l^{-1}. The dashed line obtained numerically for ideal (inviscid) water shows that the exponential decay of the transmission with sample size is mostly due to the effect of Anderson localization. In both plots, numerical data are represented by the lines of best fit only, and the data points are not shown to avoid redundancy. Green dots show the transmission of the periodic sample along the direction of broken P symmetry at frequency 386.4 kHz.

FIG. 5. Numerically calculated distribution of pressure in 16×6 periodic (a) and disordered sample (b) for frequency 453 kHz.
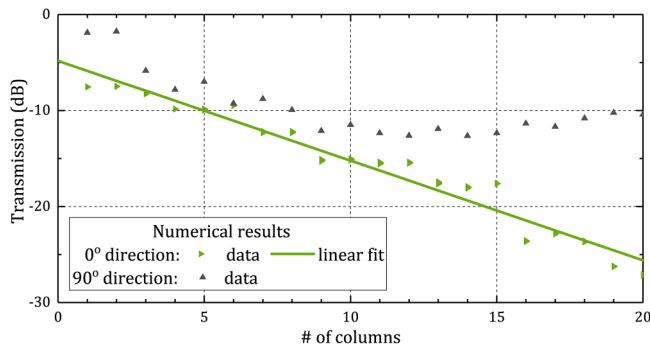
FIG. 6. Numerically calculated transmission coefficient (in dB) along the direction of disorder ($0°$, green triangles) and along the direction of order ($90°$, black triangles) as a function of the sample length. Slower than linear decay along the y axis is a clear evidence that the corresponding eigenstates are extended.

Clear evidence of Anderson localization of sound is given in Fig. 5. Here, two plots show the distribution of pressure in periodic and disordered samples. Numerical calculations for these maps were performed for inviscid fluid and hard rods, i.e., the decay of pressure with distance in the disordered sample is due solely to Anderson localization. Both distributions correspond to the same frequency of 453 kHz. According to the transmission spectra in Fig. 3 transmission through periodic and disordered samples at this frequency is relatively high. In the periodic sample, the pressure does not decay. It is seen that the maxima of pressure, related to the aforementioned interference between transmitted and reflected waves, are repeated after each four crystal periods. From the band structure in the lower panel of Fig. 3, the value of the Bloch vector at 453 kHz is approximately $k \approx 0.28\pi/a$. It is known that the transmission through a slab of thickness d oscillates because of the term $\sin^2(kd)$. The period of oscillation over d is π/k. For $k \approx 0.28a$, the period is about $3.6a$ that approximately coincides with the repetition of pressure maxima in Fig. 5(a).

We would like to stress that viscous dissipation and other factors contribute to the exponential decay of the wave propagating in a disordered medium in addition to Anderson localization. Therefore, it may sometimes be hard to separate these contributions. Moreover, if it were an electronic system, the dissipation would mean inevitable inelastic scattering which poses as a source of phase-breaking processes that destroy localization. The situation is better for classical waves since dissipation usually reduces the amplitude of the scattered wave, leaving its phase unchanged. Nevertheless, dissipation may strongly suppress Anderson localization or mislead the interpretation of experimental results.[1,24] The original method of the detection of Anderson localization in a medium with optical absorption based on analysis of electromagnetic fluctuations in transmitting channels was proposed in Ref. 3.

While dissipation plays a role in our experiments with nonreciprocal propagation of sound, its contribution to the decay of sound is quite small as compared to backscattering, which is the physical reason of localization. In Fig. 4, the dashed line shows the numerical results for transmission vs sample length in ideal inviscid water. It is clear that the slope of the dashed line is very close to

the slope of the lines obtained for viscous water. The decay of sound in inviscid water is solely due to Anderson localization. The slope of the dashed line gives the localization length $l_{ideal} = 9.66$, which is only 16% longer than that calculated for viscous water. Relatively small contribution of viscous dissipation to the exponential decay of sound is in qualitative agreement with the evaluation of the viscous propagation length given by Eq. (1).

It is interesting to compare the decay of the transmission coefficient along the x axis (disorder) and along the y axis (order). While the wave propagating along the y axis is not a standard Bloch wave, it carries information about translational periodicity and does not decay exponentially. Numerical simulation of the decay of the transmission coefficient with the sample length in Fig. 6 clearly shows that the sound intensity decays much slower than the exponential law along the y axis (black triangles) and has a tendency to saturate. Qualitatively, a different decay of the transmitted sound with the length is due to different arrangements of scatterers: disordered and ordered. Thus, we may conclude that sound propagating along the y axis is represented by extended states. These states may exhibit some signatures of wave chaos but this question requires a detailed study of the distribution of resonances within a much wider region of frequencies.

The phononic crystal used in the experiments is intentionally designed to have the maximal level of disorder, which turns out to be shorter than the length of the sample. In a sequence of disoriented rods, each rod is a strong scatterer of sound. Therefore, the elastic mean free path l_{el} is of the order of the distance between the scatterers, $l_{el} \sim a$. For the range of frequencies used in the experiments, the wavelength λ is also of the order of the period a, i.e., the Ioffe–Regel criterion of localization[24,25] $l_{el} \sim \lambda$, is satisfied. At the same time, the dissipative propagation length is long enough, $1/\gamma(\omega) \gg \lambda$, which allows multiple scattering—one more necessary condition for the observation of Anderson localization.

Aperiodic photonic crystals with structural disorder were studied numerically in Refs. 20 and 21. Elastic rods with rectangular cross section were arranged in a square lattice. The disorder was introduced along one direction by randomizing the size of the rectangles, while their orientation remains the same. Localization of elastic waves propagating along the direction of disorder has been numerically confirmed. While the dissipation of waves was not taken into account, the results for localization length obtained in Refs. 20 and 21 qualitatively agree with those shown in Figs. 4 and 6.

All the previous results were obtained for the structures with a strong disorder. It means that the angle of orientation of the scatterers fluctuates randomly from column to column. The amplitude of fluctuation was not limited, i.e., the angles of orientation were evenly distributed within the interval from $0°$ to $360°$. The case of weak disorder, when the amplitude of fluctuations is small and the scatterers are approximately oriented along a given direction, requires special attention.

The measure of disorder in a sample shown in Fig. 1 is the root mean square $\sigma = \sqrt{\langle \phi_n^2 \rangle}$ of the angle ϕ_n fluctuating with the column number n. In an ordered crystal, all the scatterers are oriented along the direction $\phi_n = 0$. In a weakly disordered sample where $\sigma \ll 1$ localization occurs at longer distances. The weak disorder can be treated perturbatively. According to Thouless,[19] the Laypunov exponent scales with σ as $l^{-1} \propto \sigma^2$. Later, it was proved
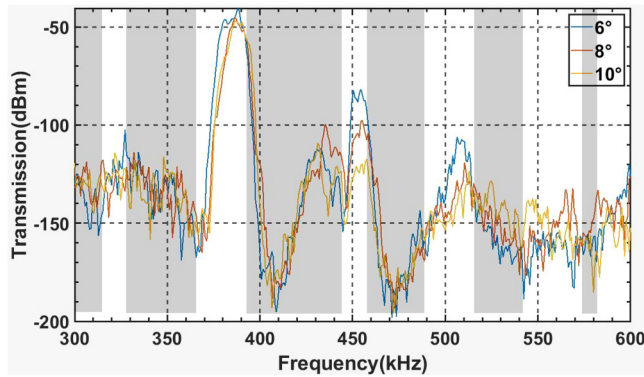
FIG. 7. Experimental transmission spectra for three weakly disordered 16×6 disordered samples with $\sigma = 6°$, $\sigma = 8°$, and $\sigma = 10°$. The regions of the gaps for infinite dissipationless phononic crystal with $\sigma = 0$ are shaded.

FIG. 8. Log–log plots for the Lyapunov exponent vs disorder for the midband (453.6 kHz) and band edge (448 kHz) frequencies. For the samples with weak disorder, the linear fit is shown by straight lines.

that this result is valid for the states lying not very close to a band edge.[26] At the band edge, the quadratic scaling is replaced by $l^{-1} \propto \sigma^{2/3}$. Such anomalous scaling of the Laypunov exponent was demonstrated analytically for the discrete disordered Anderson model,[27] for weakly disordered layered structure,[28] and for the quantum particle in slightly disordered 1D "periodic" potential.[29] Anomalous scaling at the band edge is due to the vanishing contribution to the drift term in the corresponding Fokker–Planck equation, describing wave evolution in the random medium. Stronger sensitivity to the disorder near the band edge was proposed[24] for the experimental observation of the localization of light in the 3D partially ordered medium.[30] A tendency to anomalous localization of light propagating through a weakly disordered set of dielectric layers was numerically demonstrated in Ref. 31.

While it is known that an arbitrarily weak level of 1D disorder leads to Anderson localization of waves,[2] lack of sufficiently long samples makes the observation of localization in weakly disordered samples problematic. In our experiments, we used 16×6 samples with three levels of weak disorder: $\sigma = 6°$, $\sigma = 8°$, and $\sigma = 10°$. The transmission spectra for 16×6 samples (see Fig. 1) are shown in Fig. 7. Because of the weak disorder, the transmitting bands coincide approximately with the bands of infinite dissipationless phononic crystal shown in Fig. 3. The localization length was calculated from Eq. (3) for each value of σ using the data obtained from the measurements of the decay of sound intensity with an increasing number of columns. Statistical averaging was performed over the results obtained for three different samples belonging to the statistical ensemble with the same value of σ. The analysis of scaling with σ was performed for two frequencies of 453.6 kHz (midband) and 448 kHz (band edge). The results are plotted in Fig. 8. At the midband, $l^{-1} \sim \sigma^{1.7}$ and at the band edge, $l^{-1} \sim \sigma^{0.54}$. Both exponents are less than the theoretically predicted values, $\sigma = 2$ and $\sigma = 0.67$. The main reasons for this inconsistency are not sufficiently long samples and lack of statistical averaging. One more reason is viscous losses, which are ignored in theoretical calculations. Nevertheless, the plots in Fig. 8 clearly
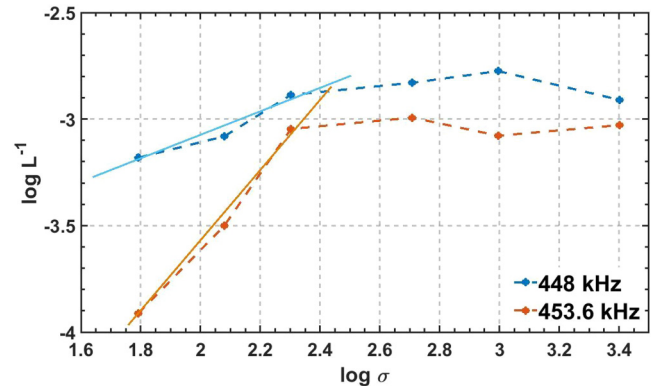
demonstrate enhanced sensitivity of the Lyapunov exponent to the level of weak disorder for the modes in the vicinity of the band edge. Very recently, a similar result has been reported for the electromagnetic modes in a waveguide formed at the interface of two slightly disordered photonic crystals.[32] We are not aware of a similar result in acoustics.

The plots in Fig. 8 also show that the transition from weak to strong disorder occurs at $\sigma \approx 15°$. For a stronger disorder, the Lyapunov exponent exhibits saturation that corresponds to the theoretical asymptotics $l^{-1} \sim \ln \sigma$ reported in Ref. 33.

IV. CONCLUSIONS

We propose a new type of the disordered phononic crystal where asymmetric solid rods are periodically arranged in the 2D lattice and the deliberate and controlled disorder is introduced due to the random orientation of each rod. This design allows the fabrication of 2D disorder, as well as of 1D disorder, where the rods of the same column are equally oriented but the columns are disoriented with respect to each other. Analysis of the transmission spectra of the phononic crystals of different lengths leads to the conclusion that sound waves propagating along disordered direction are exponentially localized but the waves running in the perpendicular direction (along periodicity) are extended, although they are not associated with standard Bloch waves in 2D lattice. Due to the different nature of the modes the proposed 2D phononic crystal with 1D disorder is an example of strongly anisotropic metamaterial with metallic behavior along the direction of order and insulating behavior along the direction of disorder. Since the phononic crystals are embedded in viscous water, the decay of sound is due to coherent backscattering that leads to Anderson localization and to viscous absorption. Our estimate shows that the contribution of the latter factor does not exceed 10%. Experimental and numerical results for the transmission and localization length are in reasonable agreement. In the regime of weak disorder, anomalous scaling of the Lyapunov exponent with the level of

disorder is experimentally confirmed for the modes in the vicinity of band edge. Standard Thouless's scaling is observed for the midband modes.

ACKNOWLEDGMENTS

DATA AVAILABILITY

The data that support the findings of this study are available from the corresponding author upon reasonable request.

REFERENCES

[1]P. W. Anderson, "The question of classical localization: A theory of white paint?," Philos. Mag. B **52**, 505 (1985).

[2]N. F. Mott and W. D. Twose, "The theory of impurity conduction," Adv. Phys. **10**, 107 (1961).

[3]A. A. Chabanov, M. Stoytchev, and A. Z. Genack, "Statistical signatures of photon localization," Nature **404**, 850 (2000).

[4]Y. Lahini, A. Avidan, F. Pozzi, M. Sorel, R. Morandotti, D. N. Christodoulides, and Y. Silberberg, "Anderson localization and nonlinearity in one-dimensional disordered photonic lattices," Phys. Rev. Lett. **100**, 013906 (2008).

[5]A. Szameit, Y. V. Kartashov, P. Zeil, F. Dreisow, M. Heinrich, R. Keil, S. Nolte, A. Tünnermann, V. A. Vysloukh, and L. Torner, "Wave localization at the boundary of disordered photonic lattices," Opt. Lett. **35**, 1172 (2010).

[6]F. Riboli, P. Barthelemy, S. Vignolini, F. Intonti, A. De Rossi, S. Combrie, and D. S. Wiersma, "Anderson localization of near-visible light in two dimensions," Opt. Lett. **36**, 127 (2011).

[7]S. Stützer, Y. V. Kartashov, V. A. Vysloukh, A. Tünnermann, S. Nolte, M. Lewenstein, L. Torner, and A. Szameit, "Anderson cross-localization," Opt. Lett. **37**, 1715 (2012).

[8]D. S. Wiersma, P. Bartolini, A. Lagendijk, and R. Righini, "Localization of light in a disordered medium," Nature **390**, 671 (1997).

[9]D. S. Wiersma, "Disordered photonics," Nat. Photonics **7**, 188 (2013).

[10]M. Segev, Y. Silberberg, and D. N. Christodoulides, "Anderson localization of light," Nat. Photonics **7**, 197 (2013).

[11]I. S. Graham, L. Piché, and M. Grant, "Experimental evidence for localization of acoustic waves in three dimensions," Phys. Rev. Lett. **64**, 3135 (1990).

[12]R. L. Weaver, "Anderson localization of ultrasound," Wave Motion **12**, 129 (1990).

[13]J. Flores, L. Gutiérrez, R. A. Méndez-Sánchez, G. Monsivais, P. Mora, and A. Morales, "Anderson localization in finite disordered vibrating rods," Europhys. Lett. **101**, 67002 (2013).

[14]J. C. Ángel, J. C. Torres-Guzmán, and A. Díaz de Anda, "Anderson localization of flexural waves in disordered elastic beams," Sci. Rep. **9**, 3572 (2019).

[15]H. Hu, A. Strybulevych, J. H. Page, S. E. Skipetrov, and B. A. van Tiggelen, "Localization of ultrasound in a three-dimensional elastic network," Nat. Phys. **4**, 945 (2008).

[16]Y. Ye, M. Ke, J. Feng, M. Wang, C. Qiu, and Z. Liu, "Transversal Anderson localization of sound in acoustic waveguide arrays," J. Phys.: Condens. Matter **27**, 155402 (2015).

[17]E. Walker, A. Neogi, A. Bozhko, Yu. Zubov, J. Arriaga, H. Heo, J. Ju, and A. A. Krokhin, "Nonreciprocal linear transmission of sound in a viscous environment with broken P symmetry," Phys. Rev. Lett. **120**, 204501 (2018).

[18]H. Heo, E. Walker, Yu. Zubov, D. Shymkiv, D. Wages, A. Krokhin, T.-Y. Choi, and A. Neogi, "Non-reciprocal acoustics in a viscous environment," Proc. R. Soc. A **476**, 657 (2020).

[19]Ill-Condensed Matter, edited by R. Balian, R. Maynard, and G. Toulouse (North-Holland, New York, 1979), p. 1; D. J. Thouless, "Electrons in disordered systems and the theory of localization," Phys. Rep. **13**, 95 (1974).

[20]Z.-Z. Yan, C. Zhang, and Y.-S. Wang, "Elastic wave localization in two-dimensional phononic crystals with one-dimensional random disorder and aperiodicity," Physica B **406**, 1154 (2011).

[21]Z.-Z. Yan and C. Zhang, "Wave localization in two-dimensional porous phononic crystals with one-dimensional aperiodicity," Ultrasonics **52**, 598 (2012).

[22]L. D. Landau and E. M. Lifshitz, Fluid Mechanics, 2nd ed. (Elsevier, Oxford, 1984).

[23]M. Ibarias, Yu. Zubov, J. Arriaga, and A. A. Krokhin, "Phononic crystal as a homogeneous viscous metamaterial," Phys. Rev. Res. **2**, 022053(R) (2020).

[24]S. John, "Electromagnetic absorption in a disordered medium near a photon mobility edge," Phys. Rev. Lett. **53**, 2169 (1984).

[25]A. Lagendijk, B. A. van Tiggelen, and D. S. Wiersma, "Fifty years of Anderson localization," Phys. Today **62**(8), 24 (2009).

[26]B. Derrida and E. Gardner, "Lyapunov exponent of the one dimensional Anderson model: Weak disorder expansions," J. Phys. **45**, 1283 (1984).

[27]F. M. Izrailev, S. Ruffo, and L. Tessieri, "Classical representation of the one-dimensional Anderson model," J. Phys. A: Math. Gen. **31**, 5263 (1998).

[28]F. M. Izrailev, A. A. Krokhin, and N. M. Makarov, "Anomalous localization in low-dimensional systems with correlated disorder," Phys. Rep. **512**, 125 (2012); J. C. Hernández-Herrejón, F. M. Izrailev, L. Tessieri, "Anomalous localization in the aperiodic Kronig–Penney model," J. Phys. A: Math. Theor. **43** 425004 (2010).

[29]Y. A. Godin, S. Molchanov, and B. Vainberg, "Wave propagation in a one-dimensional randomly perturbed periodic medium," Waves Random Complex Media **17**, 381 (2007).

[30]K. M. Douglass, S. John, T. Suezaki, G. A. Ozin, and A. Dogariu, "Anomalous flow of light near a photonic crystal pseudo-gap," Opt. Express **19**, 25320 (2011).

[31]A. R. McGurn, K. T. Christensen, F. M. Mueller, and A. A. Maradudin, "Anderson localization in one-dimensional randomly disordered optical systems that are periodic on average," Phys. Rev. B **47**, 13120 (1993).

[32]G. Arregui, J. Gomis-Bresco, C. M. Sotomayor-Torres, and P. D. Garcia, "Quantifying the robustness of topological slow light," Phys. Rev. Lett. **126**, 027403 (2021).

[33]J. L. Pichard, "The one-dimensional Anderson model: Scaling and resonances revisited," J. Phys. C: Solid State Phys. **19**, 1519 (1986).